

01 Jan 1986

## Resonant Charge Transfer In Symmetric Alkali-ion Alkali-atom Collisions

F. K. Men

M. Kimura

Ronald E. Olson

Missouri University of Science and Technology, [olson@mst.edu](mailto:olson@mst.edu)

Follow this and additional works at: [https://scholarsmine.mst.edu/phys\\_facwork](https://scholarsmine.mst.edu/phys_facwork)

 Part of the [Physics Commons](#)

---

### Recommended Citation

F. K. Men et al., "Resonant Charge Transfer In Symmetric Alkali-ion Alkali-atom Collisions," *Physical Review A*, vol. 33, no. 6, pp. 3800 - 3806, American Physical Society, Jan 1986.

The definitive version is available at <https://doi.org/10.1103/PhysRevA.33.3800>

This Article - Journal is brought to you for free and open access by Scholars' Mine. It has been accepted for inclusion in Physics Faculty Research & Creative Works by an authorized administrator of Scholars' Mine. This work is protected by U. S. Copyright Law. Unauthorized use including reproduction for redistribution requires the permission of the copyright holder. For more information, please contact [scholarsmine@mst.edu](mailto:scholarsmine@mst.edu).

## Resonant charge transfer in symmetric alkali-ion—alkali-atom collisions

F. K. Men

*Department of Physics, University of Wisconsin—Madison, Madison, Wisconsin 53706*

M. Kimura

*Joint Institute for Laboratory Astrophysics, University of Colorado and National Bureau of Standards, Boulder, Colorado 80309*

R. E. Olson

*Department of Physics, University of Missouri—Rolla, Rolla, Missouri 65401*

(Received 11 November 1985)

Resonant charge transfer in alkali-ion—alkali-atom collisions is investigated by using the molecular-orbital expansion method incorporating the use of electron translation factors. Molecular wave functions and eigenenergies are obtained by the pseudopotential method. Molecular properties,  $R_e$ ,  $D_e$ , and  $\omega_e$ , obtained in the present calculation are in good accord with other recent theoretical results, as well as spectroscopic measurements. Three-state close-coupling calculations reproduce the positions of the maxima and minima in the oscillatory structure seen experimentally in the resonant-charge-transfer cross sections for the  $\text{Li}_2^+$  and  $\text{Cs}_2^+$  systems. The magnitude of the total cross sections and their velocity dependence are in agreement with experimental measurements.

### I. INTRODUCTION

Resonant and nonresonant charge transfer in alkali-ion—alkali-atom collisions has been a popular subject both experimentally<sup>1–5</sup> and theoretically.<sup>6–18</sup> In particular, the oscillations as a function of collision energy in the total charge-transfer cross sections observed in experiments have attracted theoretical interest since the late 1960s.<sup>6–11</sup>

Another reason for such a large number of theoretical studies lies in the fact that these systems consist of one valence electron plus two closed-shell ionic cores (pseudo-one-electron system) so that various pseudopotential and model potential techniques, in addition to the *ab initio* method, can be applied to obtain accurate molecular wave functions and eigenenergies.<sup>12–18</sup> These systems, therefore, provide a convenient test for checking the quality of calculated molecular wave functions and eigenenergies since the calculated cross sections can be compared to experimental data. For these comparisons, the multistate molecular-orbital (MO) expansion method within the semiclassical formalism has been widely used for the study of inelastic events in ion-atom collisions at low-to-intermediate energies. However, as is well known, the conventional MO expansion method [or perturbed-stationary-state (PSS) method] has a fundamental defect due to its neglect of electron translation factors (ETF's). Ignorance of the ETF causes the scattering wave function not to be Galilean invariant. Thus the calculated-coupling matrix elements show an origin dependence on the electron coordinate chosen, and hence, the cross section cannot be determined uniquely. Only recently has the application of the ETF-modified MO expansion method been used successfully for the study of pseudo-one-electron ion-atom collisions in the keV-energy region.<sup>16,19,20</sup> To our knowledge, no studies of charge transfer in alkali-

ion—alkali-atom collisions have been performed using the multistate MO expansion method where the ETF effect has been incorporated correctly.<sup>21</sup>

The purpose of this paper is twofold: (i) to present molecular wave functions and eigenenergies for all the symmetric alkali-ion—alkali-atom systems (i.e.,  $\text{Li}_2^+$ ,  $\text{Na}_2^+$ ,  $\text{K}_2^+$ ,  $\text{Rb}_2^+$ , and  $\text{Cs}_2^+$ ) and (ii) to present calculated collision cross sections obtained with the ETF-modified MO-expansion method.

The charge-transfer mechanism and also the origin of the oscillatory structure seen in the charge-transfer cross section as a function of the collision energy have been investigated thoroughly<sup>6–12,16</sup> and consequently, the physical explanations of these phenomena are well known. Therefore, particular emphasis in this paper is placed on the quantitative aspects of the collision systems.

### II. THEORY

#### A. Molecular states

Alkali-ion—alkali-atom systems, which have only one valence electron that is loosely bound outside of two tight ionic cores, are regarded as pseudo-one-electron systems. Because of this condition, these systems have been chosen as an ideal example for molecular structure calculations.<sup>12–19,22,23</sup> The molecular structure calculations usually employ pseudopotential or model potential techniques to replace the potential produced by the core electrons and nucleus of the alkali atom. In our calculations, we have used an  $l$ -dependent Gaussian-type pseudopotential of the form<sup>22</sup>

$$V^P(\mathbf{r}) = \sum_{l,m} V_l(r) |Y_{lm}\rangle \langle Y_{lm}| \quad (1)$$

TABLE I. Molecular properties.

	$R_e$ ( $a_0$ )	$D_e$ (eV)	$\omega_e$ ( $\text{cm}^{-1}$ )	
$\text{Li}_2^+$	5.890	1.248	254.6	Present
	5.839	1.28	283	Ref. 26
	$5.877 \pm 0.019$	$1.2980 \pm 0.0007$	$262.2 \pm 1.5$	Ref. 29
$\text{Na}_2^+$	6.762	0.982	119.2	Present
	6.803	0.980	123	Ref. 26
	$6.803 \pm 0.094$	0.986	$120.8 \pm 0.8$	Ref. 30
$\text{K}_2^+$	8.304	0.803	67.8	Present
	8.390	0.801	75	Ref. 26
	8.315	0.794	72.5	Ref. 31
$\text{Rb}_2^+$	8.771	0.765	48.40	Present
	9.036	0.76	47	Ref. 27
	8.504	0.66		Ref. 28
$\text{Cs}_2^+$	9.765	0.686	33.58	Present
	9.883	0.71	33	Ref. 27
	9.071	0.56		Ref. 28

with

$$V_l(r) = A_l \exp(-\xi_l r^2) - \frac{\alpha_d}{2(r^2 + d^2)^2} - \frac{\alpha_q}{2(r^2 + d^2)^3} - \frac{1}{r}, \quad (2)$$

where  $|Y_{lm}\rangle$  are the spherical harmonics. The parameters  $A_l$ ,  $\xi_l$ ,  $\alpha_d$ ,  $\alpha_q$ , and  $d$  have been chosen to fit spectroscopic data. All the data used in the present calculations are tabulated in Ref. 22. The one-electron Hamiltonian is then

$$H_{\text{el}} = -\frac{1}{2} \nabla_r^2 + V^P(\mathbf{r}_A) + V^P(\mathbf{r}_B) + \frac{1}{R}, \quad (3)$$

where  $\mathbf{r}_A$  and  $\mathbf{r}_B$  are position vectors of the one electron from the two nuclei. The Schrödinger equation to be solved is then

$$H_{\text{el}} \phi_i^{\text{BO}}(\mathbf{r}, \mathbf{R}) = E_i(R) \phi_i^{\text{BO}}(\mathbf{r}, \mathbf{R}). \quad (4)$$

The electronic wave function  $\Phi_i^{\text{BO}}(\mathbf{r}, \mathbf{R})$  is approximated using a two-center expansion in terms of a linear combination of atomic orbitals (LCAO), having the form

$$\phi_i^{\text{BO}}(\mathbf{r}, \mathbf{R}) = \sum_j c_{ij} \phi_j(\mathbf{r}_A) + \sum_j d_{ij} \phi_j(\mathbf{r}_B). \quad (5)$$

Slater-type orbitals (STO's) are used as a basis with fixed orbital exponents. The basis sets and the orbital exponents used are listed in Table I of Ref. 19. For the  $^2\Sigma$  molecular states 18 STO's (9 STO's on each center) have been employed, while 16 STO's (8 STO's on each center) have been employed for the  $^2\Pi$  molecular states. The alkali-atom ( $(n-1)s$ ,  $ns$ , and  $np$  orbital exponents (where  $n$  represents the principal quantum number of the ground-state valence electron) are from Stevens *et al.*<sup>24</sup> For each alkali atom, two additional  $3d$  orbitals and one  $(n+1)s$  orbital were added and the exponents optimized for the lowest energy of the representative atomic level. With

this basis set along with the pseudopotentials, the average error in the ionization energies of the four lowest electronic levels of the alkali atoms is 0.0034 eV with the maximum deviation being 0.0081 eV. Detailed results of the calculated adiabatic potentials are deferred to Sec. III.

## B. Coupled equations

Within a semiclassical formalism, the scattering wave function is expanded in terms of the product of the Born-Oppenheimer wave function and the electron translation factor,

$$\Psi = \sum_i a_i(t) \phi_i^{\text{BO}}(\mathbf{r}, R) F_i(\mathbf{r}, R) \exp \left[ -i \int E_i(R) dt + \frac{1}{8} V^2 t \right], \quad (6)$$

where  $\phi_i^{\text{BO}}(\mathbf{r}, R)$  is the Born-Oppenheimer wave function which satisfies the Schrödinger equation in Eq. (4).  $F_i(\mathbf{r}, R)$  represents the ETF which ensures the scattering wave function [Eq. (6)] satisfies the correct boundary conditions. It has the form

$$F_i(\mathbf{r}, R) = \exp \left[ \frac{i}{2} f_i(\mathbf{r}, R) \mathbf{r} \cdot \mathbf{V} \right], \quad (7)$$

where  $\mathbf{V}$  is the relative velocity of the heavy particles and  $f_i(\mathbf{r}, R)$  is the switching function which plays a role in incorporating the two-center character into the ETF.

Substituting Eq. (6) into the time-dependent Schrödinger equation, multiplying by  $\phi_j^* \text{BO} F_j^*$  from the left, expanding the ETF in powers of  $\mathbf{V}$ , and retaining the first-order terms of  $\mathbf{V}$ , one can obtain the coupled equation for the multichannel case,

$$i \dot{a}_i(t) = \sum_{j \neq i} \mathbf{V} \cdot (\mathbf{P} + \mathbf{A})_{ji} a_j \exp \left[ -i \int^t (E_i - E_j) dt' \right], \quad (8)$$

where  $\mathbf{P}$  and  $\mathbf{A}$  are the nonadiabatic coupling and its ETF correction term, respectively. The forms are written,

$$\mathbf{P}_{ji} = \langle \phi_j^{\text{BO}} | -i\nabla_{\mathbf{R}} | \phi_i^{\text{BO}} \rangle, \quad (9)$$

$$\mathbf{A}_{ji} = i(E_j - E_i) \langle \phi_j^{\text{BO}} | \mathbf{S}_i | \phi_i^{\text{BO}} \rangle, \quad (10)$$

with

$$\mathbf{S}_i = \frac{1}{2} f_i(\mathbf{r}, \mathbf{R}) \mathbf{r}. \quad (11)$$

We have chosen the form  $f_i = \tanh(R\beta\eta)$  for the switching function, where  $\beta$  is the parameter used to minimize the coupling and  $\eta$  is the "angular" spheroidal coordinate. Details of these quantities are discussed in Ref. 25. In a rotating coordinate frame, the nonadiabatic coupling and its ETF correction terms can be divided into two contributions, namely radial coupling and rotational coupling.

The initial condition for solving the coupled equations (8) is  $a_k(-\infty) = \delta_{ik}$ , if  $i$  designates the initial state. Therefore, the probability for charge transfer in the  $k$ th state is given by

$$P_k(E; b) = |a_k(+\infty, b)|^2 \quad (12)$$

and the corresponding cross section is obtained from

$$Q_k(E) = 2\pi \int_0^\infty db b P_k(E; b). \quad (13)$$

For the calculations reported here, a linear trajectory was used to describe the heavy-particle motion. The coupled equations (8) were solved numerically with a relative truncation error between  $10^{-4}$  and  $10^{-5}$ . Simpson's method was used to calculate the cross section in Eq. (13) within the estimated accuracy of 0.1%.

For symmetric resonant-charge transfer, the two relevant molecular states are of different symmetries, namely the  $\Sigma_g$  and  $\Sigma_u$  molecular states. Therefore, these two states do not couple through the usual dynamical coupling. However, since each trajectory has a component on the two adiabatic potentials, the evolution of the phase factor as a function of time is different and induces the transition.

We can reduce Eq. (8) to the simpler two-state case. The resulting probability is then given by

$$P(E, b) = \sin^2(\frac{1}{2}\phi) \quad (14)$$

with

$$\phi = \int_{-\infty}^{\infty} (E_g - E_u) dt. \quad (15)$$

The total cross section can be calculated by Eq. (13) as before.

### III. RESULTS AND DISCUSSION

#### A. Adiabatic potentials

Adiabatic potential curves for the  $\text{Li}_2^+$ ,  $\text{Na}_2^+$ ,  $\text{K}_2^+$ ,  $\text{Rb}_2^+$ , and  $\text{Cs}_2^+$  systems are shown in Figs. 1–5, respectively, calculated by the pseudopotential method described in Sec. II A. The two lowest-energy curves,  $1^2\Sigma_g$  and  $1^2\Sigma_u$  states, dissociate to a ground-state alkali-alkali-atom pair at infinite internuclear separation. The first excited level corresponds to the alkali-ion +

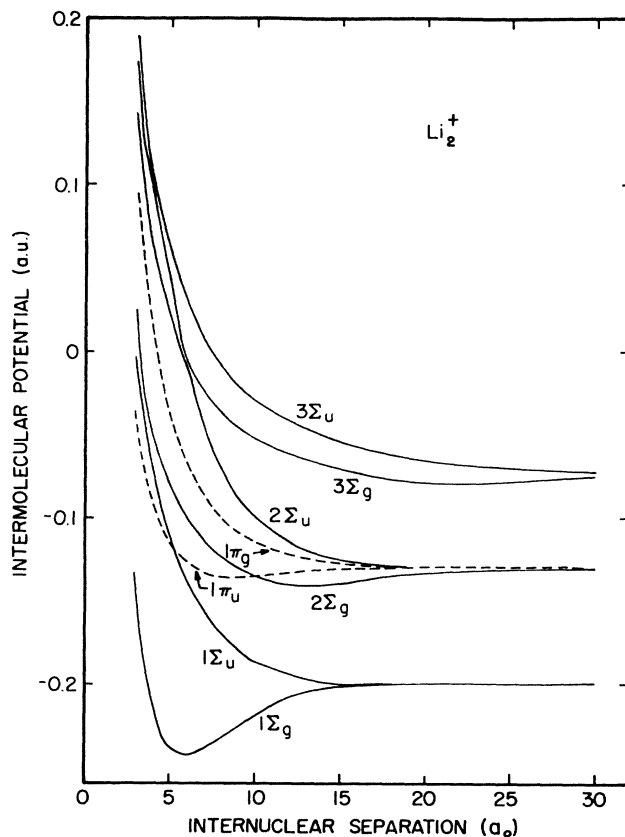


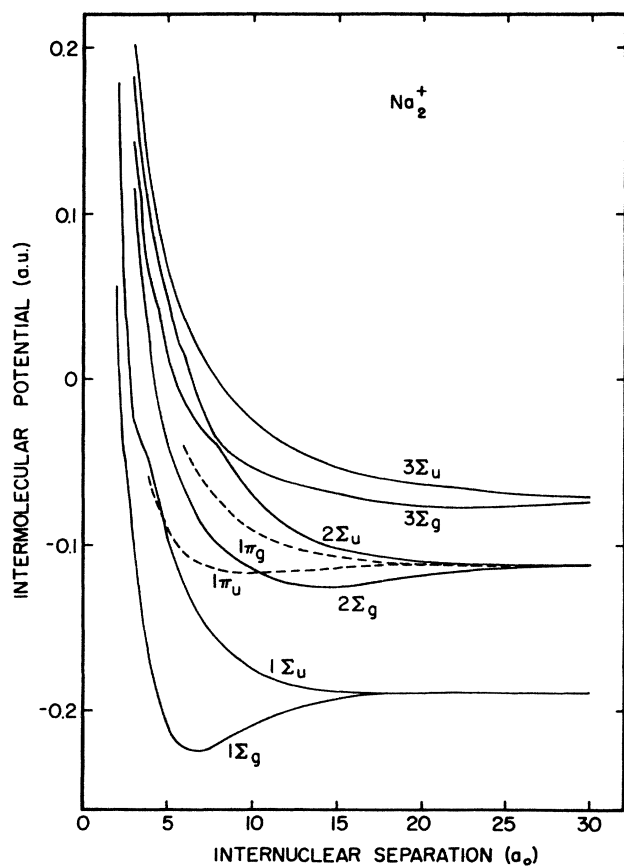
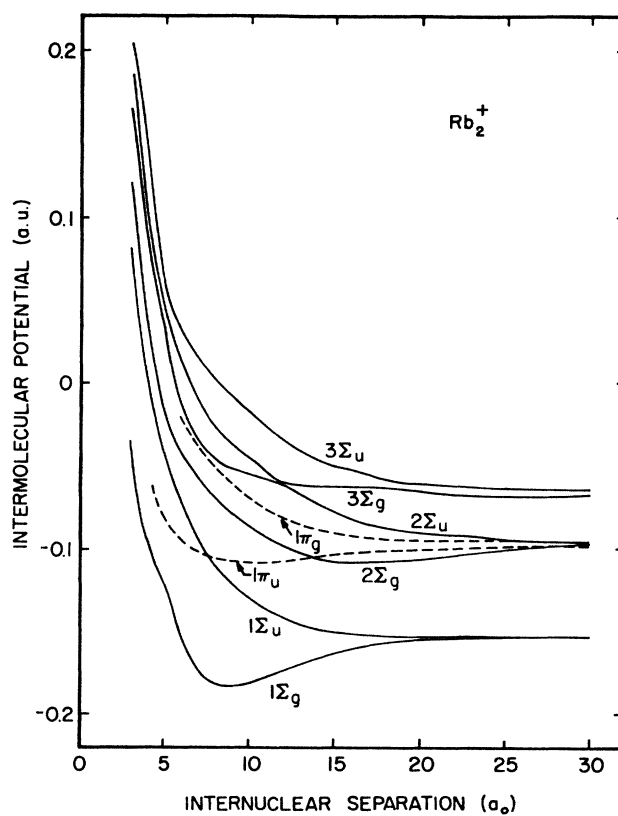
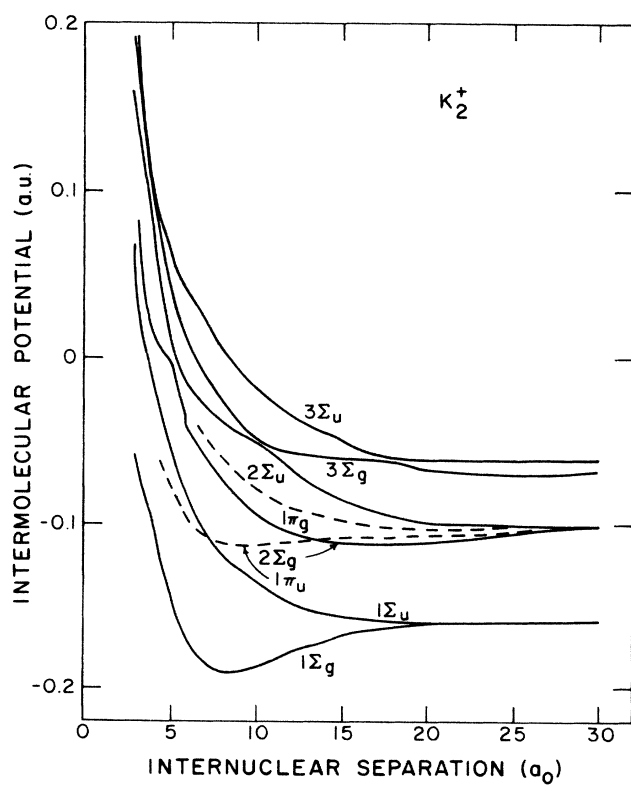
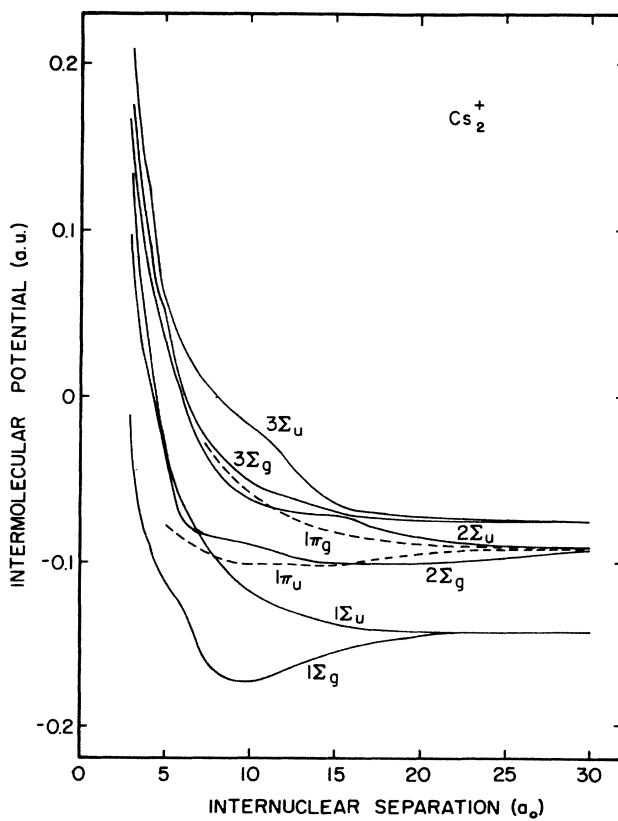
FIG. 1. Adiabatic potential curves for  $\text{Li}_2^+$ . The solid lines represent  $^2\Sigma$  molecular states and the dashed lines represent  $^2\Pi$  molecular states.

alkali-atom ( $np$ ) state (where  $n$  represents the principal quantum number of the ground state). Regardless of the system considered, the  $1\Pi_u$  state crosses the  $1\Sigma_u$  state at  $R \leq 10$  a.u. This  $\Sigma$ - $\Pi$  curve crossing plays an important role for the charge-transfer mechanism through rotational coupling at the higher collision energies.

We have calculated the equilibrium distance  $R_e$ , the dissociation energy  $D_e$ , and the vibrational frequency  $\omega_e$  of the ground  $1^2\Sigma_g$  states. The results are listed in Table I. Results of other theoretical work<sup>26–28</sup> on these molecular quantities are also listed in Table I for comparison.

The model potential calculations for  $\text{Li}_2^+$ ,  $\text{Na}_2^+$ , and  $\text{K}_2^+$  by Henriët and Masnau-Seeuws,<sup>26</sup> who used a large basis set (more than 67 orbitals for each center), are considered to be the most elaborate calculation for these systems to date. Agreement between our results for  $R_e$  and  $D_e$  values of  $\text{Li}_2^+$ ,  $\text{Na}_2^+$ , and  $\text{K}_2^+$  systems and those of Henriët and Masnau-Seeuws<sup>26</sup> is very good—within a few percent. However, the agreement for the  $\omega_e$  value is usually not as good, with differences being on the order of 10%. Good agreement between our results and the *ab initio* calculation by Henderson *et al.*<sup>14</sup> is also found for the  $\text{Li}_2^+$  system. For these three systems, our results for the above molecular quantities are in good accord with measurements.<sup>29–31</sup>

In contrast to the ample theoretical as well as experimental studies of molecular spectroscopy on the above three systems, studies on  $\text{Rb}_2^+$  and  $\text{Cs}_2^+$  are scarce. The

FIG. 2. Adiabatic potential curves for  $\text{Na}_2^+$ .FIG. 4. Adiabatic potential curves for  $\text{Rb}_2^+$ .FIG. 3. Adiabatic potential curves for  $\text{K}_2^+$ .FIG. 5. Adiabatic potential curves for  $\text{Cs}_2^+$ .

theoretical result of von Szentpaly *et al.*<sup>27</sup> who used a semiempirical pseudopotential method seems to be one of the most accurate calculations of this kind. Agreement of our results with those of von Szentpaly *et al.*<sup>27</sup> for both systems is satisfactory with the maximum discrepancy being less than 4% for the  $D_e$  value of the  $\text{Rb}_2^+$  case. The theoretical result calculated by Valance<sup>28</sup> who employed the model potential method is also shown in Table I. His results are appreciably smaller in both  $R_e$  and  $D_e$  values for both the  $\text{Rb}_2^+$  and  $\text{Cs}_2^+$  systems.

As a whole, our pseudopotential calculations that used relatively small basis sets gave reasonably accurate ground-state potential curves. For the low-lying excited states there are no experimental data to check the precision of our calculated results except for the asymptotic values which are within 0.01% of the spectroscopic data.

## B. Cross sections

### 1. Two-state calculation

Resonant charge-transfer cross sections for all the symmetric alkali-ion-alkali-atom collisions have been calculated by using Eqs. (14) and (15) with Eq. (13) in the two-state MO expansion method. Results are shown in Figs. 6–10 as a function of inverse velocity. The general trends of the cross sections for all systems seen in the figures are the following.

(a) Notable oscillatory structure of the cross sections as a function of the inverse velocity. Smith *et al.*<sup>6,11</sup> have explained this characteristic feature as due to the combined effect of a maximum in the interaction potential difference and a large repulsive core. The oscillatory cross section can be expressed analytically as a function of

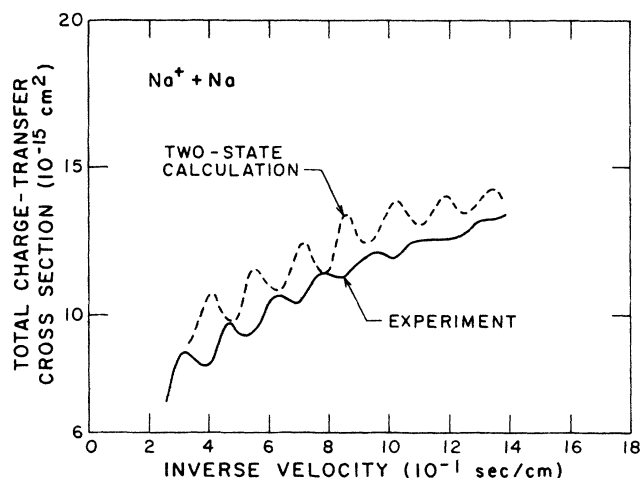


FIG. 7. Resonant charge-transfer cross section in the  $\text{Na}^+ + \text{Na}$  collision. Solid curve is experiment (Ref. 5); dashed curve is present two-state calculation.

impact velocity  $v$  in the form

$$\sigma(v) = \bar{\sigma}(v) - \alpha(v) \cos(\pi\beta v^{-1} - \delta),$$

where  $\bar{\sigma}(v)$  is the mean cross section,  $\alpha$  and  $\beta$  are slowly varying monotonic functions of  $v$ , and  $\delta$  is a phase constant, the value of which depends on the features of the interaction which give rise to the oscillations.

(b) The oscillatory structure in the measured cross section is more pronounced in the high-energy region.

(c) The magnitude of the cross section decreases as  $Z$  of the alkali-atom decreases. This is consistent with the magnitude of the energy difference between the ground gerade and ungerade states. Also, the cross section decreases as the collision energy increases as in the typical case of the resonant charge transfer.

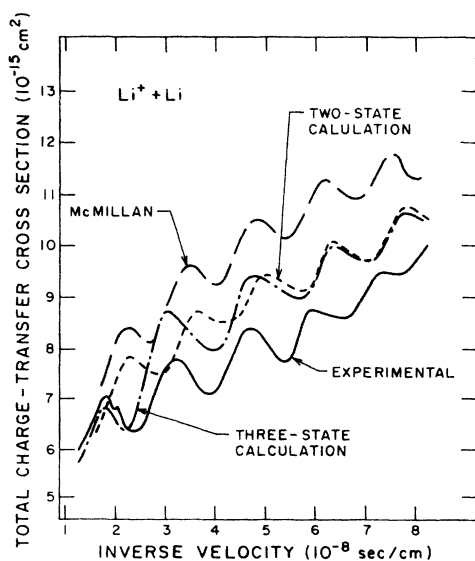


FIG. 6. Resonant-charge-transfer cross section in the  $\text{Li}^+ + \text{Li}$  collision as a function of inverse velocity. Solid curve is experiment (Ref. 1). Present two- and three-state calculations are labeled. Long-dashed curves represent theory of McMillan (Ref. 12).

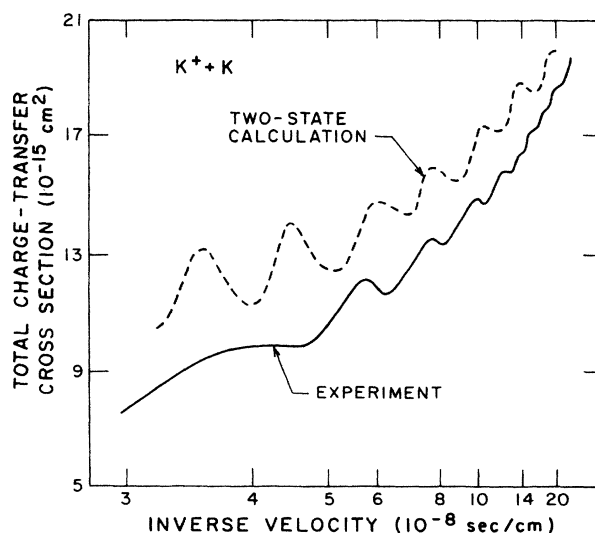


FIG. 8. Resonant-charge-transfer cross section in the  $\text{K}^+ + \text{K}$  collision. Solid curve is experiment (Ref. 5); dashed curve is present two-state calculation.

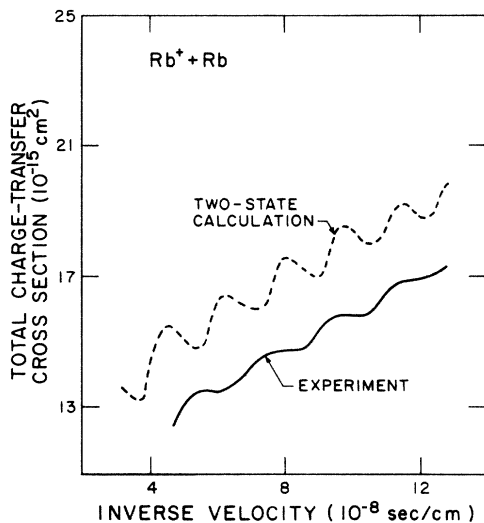


FIG. 9. Resonant-charge-transfer cross section in the  $\text{Rb}^+ + \text{Rb}$  collision. Solid curve is experiment (Ref. 5); dashed curve is present two-state calculation.

(d) The energy dependence of our calculated cross sections in the two-state approximation is in good agreement with the measurement, while the magnitude is about 15% larger than the observation. The difference in the absolute magnitude of the cross sections is outside the quoted experimental uncertainty of  $\pm 8\%$ . However, it is not clear whether the experimental arrangement could detect the charge-transfer products produced in small impact-parameter collisions (i.e., scattered to large angles). The calculated oscillatory structure is out of phase with the experimental results.

(e) For the  $\text{Li}_2^+$  case, the present result is in better accord with the measurement than that obtained by McMillan<sup>12</sup> previously. This holds also for the  $\text{Na}_2^+$  case in comparison to the previous calculation by Bottcher *et al.*<sup>13</sup> As a whole, except for the position of the maximum and minimum of the oscillatory structure in the cross section, the present calculated results agree satisfactorily with measurements.

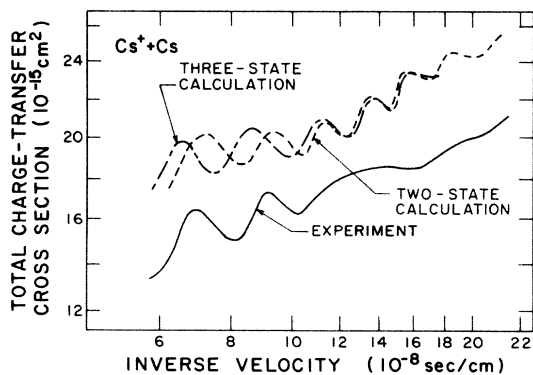


FIG. 10. Resonant-charge-transfer cross section in the  $\text{Cs}^+ + \text{Cs}$  collision. Solid curve is experiment (Ref. 5). Present two- and three-state calculations are labeled.

## 2. Three-state calculation

In the two-state calculation reported in the previous section, only the  $1\Sigma_g$  and  $1\Sigma_u$  states were adopted in the close-coupling formulation. This approximation is certainly valid in the low-energy collision. However, as the collision energy increases, the role of the  $1\Pi_u$  increases due to the possibility of inelastic transitions at the  $1\Sigma_u$ - $1\Pi_u$  curve crossing. Therefore, it is undoubtedly necessary to extend our scattering basis set in the close-coupling formula beyond the resonant states in order to understand the collision dynamics more precisely. Rewriting Eq. (8) to incorporate the rotational coupling between the  $1\Sigma_u$  and  $1\Pi_u$  states, one can obtain the three-state coupled equations, specifically, for the present case, viz.,

$$\begin{aligned}
 i\dot{a}_{\Sigma_g} &= 0, \\
 i\dot{a}_{\Sigma_u} &= \dot{\theta} \langle \Sigma_u | (P+A)^\theta | \Pi_u \rangle a_{\Pi_u} \\
 &\quad \times \exp \left[ -i \int^t (E_{\Sigma_u} - E_{\Pi_u}) dt' \right], \\
 i\dot{a}_{\Pi_u} &= \dot{\theta} \langle \Pi_u | (P+A)^\theta | \Sigma_u \rangle a_{\Sigma_u} \\
 &\quad \times \exp \left[ -i \int^t (E_{\Pi_u} - E_{\Sigma_u}) dt' \right],
 \end{aligned} \tag{16}$$

where  $(P+A)^\theta$  represents the rotational coupling operator and corresponding ETF correction operator, and  $\dot{\theta}$  denotes the angular velocity. The square of addition or subtraction of  $\Sigma_g$  and  $\Sigma_u$  scattering amplitudes obtained from Eq. (16) gives elastic or charge-transfer probabilities. Then, Eq. (13) can be used to compute cross sections.

As examples, the  $\text{Li}_2^+$  and  $\text{Cs}_2^+$  systems were selected for this study. Calculated results are displayed in Figs. 6 and 10. The most remarkable difference in the three-state calculation from the two-state result is the fact that the positions of the oscillations shift; in particular, it is now out-of-phase with the two-state result (or in-phase with the experiment) in the high-energy region. However, as expected, the three-state result approaches the two-state result as the energy decreases. The magnitude of the cross section is hardly affected by the addition of the  $1\Pi_u$  state in the calculation. This is attributed to the fact that the total resonant-charge-transfer cross section is determined by distant collisions,  $R \sim 15$  a.u., while the inelastic channel is important only at small  $R \leq 7$  a.u. where the  $1\Sigma_u$  and  $1\Pi_u$  rotational coupling is taking place. Thus the inclusion of the  $np$  inelastic channel did not improve the agreement with experiment as to the absolute magnitude of the cross sections.

The phase of the oscillations in the resonant-charge-transfer cross section found in the three-state calculation are now in good accord with the measurement for both  $\text{Li}_2^+$  and  $\text{Cs}_2^+$ . The phase of the calculated oscillations are governed by two factors: (i) the potential difference between the  $1\Sigma_g$  and  $1\Sigma_u$  state at  $R \leq 10$  a.u. and (ii) the inclusion of the other dominant channels except for the resonant channels ( $1\Pi_u$  in the present case). Good agreement of our results with the experiment seem to confirm points raised above. The better accord of  $\text{Li}_2^+$  and  $\text{Na}_2^+$  systems with the measurement than those reported previ-

ously<sup>12,13</sup> suggests that the wave functions and eigenenergies calculated in this report may be more accurate. In the previous calculations of Refs. 12 and 13, the ETF effect was neglected. However, the ETF correction form in Eq. (16) seems to be less important around the curve-crossing region in the present systems. Therefore, the quality of the wave function might be solely responsible for this discrepancy found in the various theories.

#### IV. CONCLUDING REMARKS

Accurate molecular wave functions and eigenenergies for the  $\text{Li}_2^+$ ,  $\text{Na}_2^+$ ,  $\text{K}_2^+$ ,  $\text{Rb}_2^+$ , and  $\text{Cs}_2^+$  systems were obtained by the pseudopotential method. Two- and three-state close-coupling calculations have been carried

out to investigate the resonant-charge-transfer mechanisms as well as to check the accuracy of the wave functions obtained. The oscillatory structure observed in the experiment was well reproduced in the present three-state calculations for the  $\text{Li}_2^+$  and  $\text{Cs}_2^+$  systems. These calculations confirmed the accuracy of the wave functions along with the direct comparisons to experimental values for  $R_e$ ,  $D_e$ , and  $\omega_e$ . The two-state scattering calculations agreed with the three-state ones as to magnitude of the cross sections, differing only in the oscillation frequency at the higher velocities.

#### ACKNOWLEDGMENTS

This work was supported by the Magnetic Fusion Program, U.S. Department of Energy.

- 
- <sup>1</sup>J. Perel, R. H. Vernon, and H. L. Daley, *Phys. Rev.* **138**, A937 (1965).
- <sup>2</sup>J. Perel, R. H. Vernon, and H. L. Daley, *Proceedings of the Fourth International Conference on the Physics of Electronic and Atomic Collisions, Quebec, 1965*, edited by L. Kerwin and W. Fite (Science Bookcrafters, Hastings-on-Hudson, 1965), p. 336.
- <sup>3</sup>D. C. Lorentz, G. Black, and O. Heinz, *Phys. Rev.* **137**, A1049 (1965).
- <sup>4</sup>L. L. Mario, *Phys. Rev.* **152**, 46 (1966).
- <sup>5</sup>H. L. Daley and J. Perel, *Abstracts of Papers, Sixth International Conference on the Physics of Electronic and Atomic Collisions, Cambridge, Mass., 1969*, edited by I. Amdur (MIT, Cambridge, Mass., 1969), p. 1051.
- <sup>6</sup>F. J. Smith, *Phys. Lett.* **20**, 271 (1966).
- <sup>7</sup>J. M. Peek, T. A. Green, J. Perel, and H. H. Michels, *Phys. Lett.* **20**, 1419 (1968).
- <sup>8</sup>J. Perel, H. L. Daley, J. M. Peek, and T. A. Green, *Phys. Rev. Lett.* **23**, 677 (1969).
- <sup>9</sup>R. E. Olson, *Phys. Rev.* **187**, 153 (1969).
- <sup>10</sup>J. Perel, *Phys. Rev. A* **1**, 369 (1970).
- <sup>11</sup>J. Perel, H. L. Daley, and F. J. Smith, *Phys. Rev. A* **1**, 1626 (1970).
- <sup>12</sup>W. L. McMillan, *Phys. Rev. A* **4**, 69 (1971).
- <sup>13</sup>(a) C. Bottcher, A. C. Allison, and A. Dalgarno, *Chem. Phys. Lett.* **11**, 307 (1971); (b) C. Bottcher and A. Dalgarno, *ibid.* **36**, 137 (1975).
- <sup>14</sup>G. A. Henderson, W. T. Zemke, and A. C. Wahl, *J. Chem. Phys.* **58**, 2654 (1973).
- <sup>15</sup>D. A. Hasman, *Chem. Phys. Lett.* **29**, 260 (1974).
- <sup>16</sup>C. F. Melius and W. A. Goddard III, *Phys. Rev. A* **10**, 1541 (1974).
- <sup>17</sup>(a) J. N. Bardsley, B. R. Junker, and D. W. Norcross, *Chem. Phys. Lett.* **37**, 502 (1976); (b) S. Sinha and J. N. Bardsley, *Phys. Rev. A* **14**, 104 (1976).
- <sup>18</sup>W. Muller and M. Jungen, *Chem. Phys. Lett.* **40**, 199 (1976).
- <sup>19</sup>M. Kimura, R. E. Olson, and J. Pascale, *Phys. Rev. A* **26**, 3113 (1982).
- <sup>20</sup>H. Sato, M. Kimura, A. Wetmore, and R. E. Olson, *J. Phys. B* **16**, 3037 (1983).
- <sup>21</sup>(a) N. Shimakura, H. Inouye, F. Koike, and T. Watanabe, *J. Phys. B* **14**, 2203 (1981); **17**, 2687 (1984), studied the symmetric  $\text{Li}^+ + \text{Li}$  collision by using the MO + ETF method. However, this group concerned itself mainly with the differential cross section and hence, unfortunately, did not report the resonant charge-transfer cross section. (b) The multistate MO calculation by Melius and Goddard (Ref. 13) included "ETF effect" in some sense to study  $\text{Li}^+ + \text{Na}$  collisions. However, this treatment of the ETF is considered to be not appropriate [see A. Riela and A. Salin, *J. Phys. B* **9**, 2877 (1976)].
- <sup>22</sup>J. N. Bardsley, *Case Stud. At. Phys.* **4**, 299 (1974).
- <sup>23</sup>As the most recent reference, see A. Henriët and F. Masnau-Seeuws, *Chem. Phys. Lett.* **101**, 535 (1983). This paper also includes extensive references in this field.
- <sup>24</sup>W. J. Stevens, A. M. Karo, and J. R. Hiskes, *J. Chem. Phys.* **74**, 3989 (1981).
- <sup>25</sup>M. Kimura and W. R. Thorson, *Phys. Rev. A* **24**, 3014 (1981).
- <sup>26</sup>A. Henriët and F. Masnau-Seeuws, *Chem. Phys. Lett.* **101**, 535 (1983).
- <sup>27</sup>L. von Szentpaly, P. Frenteaiba, H. Preuss, and H. Stoll, *Chem. Phys. Lett.* **93**, 555 (1982).
- <sup>28</sup>A. Valance, *J. Chem. Phys.* **69**, 355 (1978).
- <sup>29</sup>R. A. Bernheim, L. P. Gold, and T. Tipton, *J. Chem. Phys.* **78**, 2625 (1983).
- <sup>30</sup>S. Martin, J. Chevalyere, S. Valigrat, J. P. Perron, M. Broyer, M. Cabaud, and A. Hoareau, *Chem. Phys. Lett.* **87**, 235 (1982).
- <sup>31</sup>S. Leutwyler, A. Hermann, L. Wöste, and E. Schumacher, *Chem. Phys. Lett.* **48**, 253 (1980).